Perfect Lattice Actions for Staggered Fermions [1]

W. Bietenholz[a], R. Brower[b], S. Chandrasekharan[c] and U.-J. Wiese[c]

[a] HLRZ c/o KFA Jülich
52425 Jülich, Germany

[b] Department of Physics
Boston University
Boston MA 02215, USA

[c] Center for Theoretical Physics
Laboratory for Nuclear Science and Department of Physics
Massachusetts Institute of Technology
Cambridge MA 02139, USA

Preprint MIT-CTP 2584, HLRZ 74/96

We construct a perfect lattice action for staggered fermions by blocking from the continuum. The locality, spectrum and pressure of such perfect staggered fermions are discussed. We also derive a consistent fixed point action for free gauge fields and discuss its locality as well as the resulting static quark-antiquark potential. This provides a basis for the construction of (classically) perfect lattice actions for QCD using staggered fermions.

[1]This work is supported in part by funds provided by the U.S. Department of Energy (D.O.E.) under cooperative research agreement DE-FC02-94ER40818.

1 Introduction

Recently there has been a surge of interest in lattice actions which are closer to the continuum limit than standard lattice actions, in the sense that artifacts due to the finite lattice spacing are suppressed. The hope is that such improved actions will allow Monte Carlo simulations to reach the scaling region even on rather coarse lattices.

Based on renormalization group concepts, it has been known for a long time that perfect actions, i.e. lattice actions without any cutoff artifacts, do exist [1]. However, it is very difficult to construct – or even approximate – such perfect actions. Recent progress is based on the observation that for asymptotically free theories the determination of the fixed point action (FPA) is a classical field theory problem [2]. At infinite correlation length, a FPA is perfect. Away from the critical surface, this is in general not the case any more; at finite correlation length, FPAs are referred to as "classically perfect actions". However, they are considered as promising improved actions even at moderate correlation length. In particular, the deviations from the (quantum) perfect renormalized trajectory are likely to set in only at the two loop level [4, 5]. Indeed, a drastically improved scaling behavior of the fixed point action has been observed in some asymptotically free models [2, 3, 4], and is especially hoped for in QCD.

A classically perfect action can be constructed as a fixed point of a block variable renormalization group transformation (RGT). Usually one fixes a finite blocking factor n and builds block variables on a coarse lattice of spacing n, determined by a fine lattice with unit spacing. Then one expresses all quantities in the new lattice units, i.e. one rescales the coarse lattice back to unit spacing. At infinite correlation length and for suitable RGT parameters, an infinite number of iterations of this RGT step leads to a finite FPA. For most interacting theories, this scheme is the only way to construct FPA's non-perturbatively. There one has to perform the blocking transformation numerically (and hope for swift convergence).

For free or perturbatively interacting theories this construction can also be achieved in only one step, by a technique that we call "blocking from the continuum". This method proceeds analytically in momentum space. It has been applied to construct perturbatively perfect lattice actions for the Schwinger model and for QCD, using fixed point fermions of the Wilson type [6, 7]. In this paper we present a number of ingredients for the construction

of a classically perfect QCD lattice action with staggered fermions, using the same technique. This provides a construction scheme alternative to Ref. [7]. A motivation is that staggered fermions are particularly useful for the study of chiral symmetry breaking.

In section 2 we derive the perfect action for free staggered fermions by blocking from the continuum. In section 3 we discuss the dispersion relation and the pressure of such fixed point fermions with and without truncation. In section 4 we show how to block the gauge field consistently and we arrive at the corresponding FPA for free gauge fields. This implies a "classically perfect" static quark-antiquark potential, which is compared to the (perfect) Coulomb potential in section 5. Section 6 contains our conclusions and an outlook on possible applications.

A synopsis of the results presented here is included in Ref. [8], where we also illustrate the perturbative blocking from the continuum and where we outline how perturbatively perfect actions can serve as starting points for the non-perturbative search for FPA's.

2 Perfect free staggered fermions

The fixed point action for free, massless staggered fermions in two dimensions has been derived before [9, 3]. That derivation used a block factor 3 RGT, which does not mix the pseudoflavors [10], and which could be iterated analytically an infinite number of times. We are going to show how one can reproduce this result in one step by blocking from the continuum. [2] We also generalize the result to higher dimensions and to arbitrary masses, so we obtain an entire renormalized trajectory for free fermions.

First we introduce our notation for staggered fermions. We divide the lattice into disjoint hypercubes with centers x. Our lattice has spacing $1/2$, such that these centers have spacing 1. Each hypercube carries a set of 2^d fermionic and antifermionic pseudoflavors on its corners, where the dimension d is assumed to be even. We denote those Grassmann variables as χ_x^ρ, $\bar{\chi}_x^\rho$,

[2] This has also been achieved by H. Dilger, in a way which emphasizes the relationship to Dirac-Kähler fermions [11]. A similar suggestion occurred earlier in Ref. [12]. As a further approach one could first construct perfect naiv fermions, including all the doublers, and then build perfect staggered fermions from them. We thank M.-P. Lombardo for this remark.

where ρ is the vector pointing from the cell center x to the corner, where the variable lives. Hence the standard action for free staggered fermions reads

$$S_{st}[\bar{\chi},\chi] = \sum_{x\in\mathbb{Z}^d,\rho\rho'} \bar{\chi}^\rho_x \Big[\sum_{\mu=1}^{d} \Big(\Gamma^{\rho\rho'}_\mu \hat{\partial}_\mu + \frac{1}{2}\Gamma^{\rho\rho'}_{5\mu}\hat{\partial}^2_\mu \Big) + 2m\delta^{\rho\rho'} \Big] \chi^{\rho'}_x , \tag{2.1}$$

where we have defined the following quantities

$$\begin{aligned}
\Gamma^{\rho\rho'}_\mu &= [\delta^{\rho-\hat{\mu}/2,\rho'} + \delta^{\rho+\hat{\mu}/2,\rho'}]\sigma_\mu(\hat{\rho}), \\
\Gamma^{\rho\rho'}_{5\mu} &= [\delta^{\rho-\hat{\mu}/2,\rho'} - \delta^{\rho+\hat{\mu}/2,\rho'}]\sigma_\mu(\hat{\rho}), \\
\sigma_\mu(x) &= \begin{cases} 1 & \sum_{\nu<\mu} x_\nu \ \text{ even} \\ -1 & \text{otherwise} \end{cases} \\
\hat{\partial}_\mu \chi^\rho_x &= \frac{1}{2}(\chi^\rho_{x+\hat{\mu}} - \chi^\rho_{x-\hat{\mu}}), \\
\hat{\partial}^2_\mu \chi^\rho_x &= \chi^\rho_{x+\hat{\mu}} + \chi^\rho_{x-\hat{\mu}} - 2\chi^\rho_x .
\end{aligned} \tag{2.2}$$

Now we are going to construct a perfect action for free staggered fermions. Instead of iterating an RGT with a finite blocking factor, we send the blocking factor to infinity and perform only one RGT. This amounts to the "blocking from the continuum": one starts from continuum fields and defines lattice variables by integrating over the unit hypercube around the corresponding lattice site. In particular, for staggered fermions we also have to take care of the flavor structure. We have to transform the continuum flavors into staggered pseudoflavors and integrate over regions, which depend on the pseudoflavor. Those regions are overlapping unit hypercubes.

It is well-known how to transform fermionic pseudoflavors in the continuum limit into flavors by a unitary transformation. We assume that the inverse of this transformation has been carried out and we start in the continuum with space filling fermionic fields $\psi,\ \bar{\psi}$, composed of pseudoflavors. Then we build staggered lattice fermions as

$$\chi^\rho_x = \int_{c_{x+\rho}} d^d y\ \psi^\rho(y)\ , \quad \bar{\chi}^\rho_x = \int_{c_{x+\rho}} d^d y\ \bar{\psi}^\rho(y)\ , \tag{2.3}$$

where c_z is a unit hypercube with center z. We define

$$\Pi(p) = \int_{c_0} d^d y \exp(ipy) = \prod_{\mu=1}^{d} \frac{\hat{p}_\mu}{p_\mu}\ ; \quad \hat{p}_\mu = 2\sin(p_\mu/2), \tag{2.4}$$

and obtain in momentum space

$$\begin{aligned}\chi^\rho(p) &= \sum_{l\in\mathbb{Z}^d} \psi^\rho(p+2\pi l)\Pi(p+2\pi l)e^{i(p+2\pi l)\rho} \\ &= \sum_{l\in\mathbb{Z}^d} \psi^\rho(p+2\pi l)\Pi^\rho(p+2\pi l), \end{aligned} \tag{2.5}$$

where

$$\Pi^\rho(p) = e^{ip\rho}\Pi(p) \tag{2.6}$$

and p is in the Brillouin zone $B =]-\pi,\pi]^d$. In analogy to Refs. [9, 3] we choose the following RGT,

$$\begin{aligned} e^{-S[\bar\chi,\chi]} &= \int \mathcal{D}\bar\psi\mathcal{D}\psi\mathcal{D}\bar\eta\mathcal{D}\eta \exp\Big\{ - s[\bar\psi,\psi] \\ &+ \frac{1}{(2\pi)^d}\int_B d^dp\Big([\bar\chi^\rho(-p) - \sum_{l\in\mathbb{Z}^d}\bar\psi^\rho(-p-2\pi l)\Pi^\rho(-p-2\pi l)]\eta^\rho(p) \\ &\quad +\bar\eta^\rho(-p)[\chi^\rho(p) - \sum_{l\in\mathbb{Z}^d}\Pi^\rho(p+2\pi l)\psi^\rho(p+2\pi l)] \\ &\quad +\bar\eta^\rho(-p)A^{\rho\rho'}\eta^{\rho'}(p)\Big)\Big\}, \end{aligned} \tag{2.7}$$

where the summation over ρ,ρ' is understood. Here $s[\bar\psi,\psi]$ is the continuum action and $\bar\eta^\rho,\ \eta^\rho$ are auxiliary staggered Grassmann fields living on the same lattice sites as $\bar\chi^\rho$ and χ^ρ. We do not enforce the blocking relation (2.5) by a δ-function, but only by a smoothly peaked function; the δ-function is smeared to a Gaussian by the matrix A. For the latter we make the ansatz,

$$A^{\rho\rho'} = a\delta^{\rho\rho'} - ic\hat p_\mu \Gamma_\mu^{\rho\rho'} e^{ip(\rho-\rho')}, \tag{2.8}$$

where a and c are referred to as mass-like and kinetic smearing parameter. They can be tuned to optimize the locality of the perfect action. In particular for $a = 0$ the RGT preserves the remnant chiral symmetry $U(1)\otimes U(1)$ (at $m = 0$), which is therefore explicitly present in the perfect action.

Integrating the RGT (2.7) we obtain the perfect lattice action

$$S[\bar\chi,\chi] = \frac{1}{(2\pi)^d}\int_B d^dp\ \bar\chi^\rho(-p)[\Delta^f(p)^{-1}]^{\rho\rho'}\chi^{\rho'}(p), \tag{2.9}$$

with the free propagator

$$\begin{aligned}\Delta^f(p)^{\rho\rho'} &= \sum_{l\in\mathbb{Z}^d} \Pi^\rho(p+2\pi l)\frac{1}{i(p_\mu+2\pi l_\mu)\gamma_\mu+m}\Pi^{\rho'}(p+2\pi l)+A^{\rho\rho'} \\ &= -i\alpha_\mu(p)\Gamma_\mu^{\rho\rho'}e^{ip(\rho-\rho')}+\beta(p)\delta^{\rho\rho'}, \end{aligned} \tag{2.10}$$

where $\alpha_\mu(p)$ and $\beta(p)$ are given by

$$\begin{aligned}\alpha_\mu(p) &= \sum_{l\in\mathbb{Z}^d}\frac{(-1)^{l_\mu}(p_\mu+2\pi l_\mu)}{(p+2\pi l)^2+m^2}\Pi(p+2\pi l)^2+c\hat{p}_\mu, \\ \beta(p) &= \sum_{l\in\mathbb{Z}^d}\frac{m}{(p+2\pi l)^2+m^2}\Pi(p+2\pi l)^2+a. \end{aligned} \tag{2.11}$$

For $p=(p_1,0,\ldots,0)$, i.e. in the effectively one dimensional case, the sum over l collapses to a sum over $l_1\in\mathbb{Z}$, which can be computed analytically. In this case, it turns out that for

$$a=\frac{\sinh(m)-m}{m^2}\ ;\quad c=\frac{\cosh(m/2)-1}{m^2}, \tag{2.12}$$

the action turns into the standard action, which is *ultralocal*; the range of couplings does not exceed nearest neighbors. In higher dimensions the sum over l has to be done numerically and we can only obtain locality in the sense of an exponential decay. It turns out that the same choice of smearing parameters a and c still yields an extremely local action, i.e. the exponential decay is extremely fast, in analogy to our observations for Wilson fermions [7, 9]. Hence we are going to use the smearing parameters given in eq. (2.12) in any dimension.

In the chiral limit $m=0$ this result coincides with the FPA obtained in Refs. [9, 3]. The optimally tuned value of a vanishes in this limit, [3] hence we obtain in the massless case an extremely local perfect action, which still has the remnant chiral symmetry.

The inverse propagator can be represented as

$$\begin{aligned}[\Delta^f(p)^{-1}]^{\rho\rho'} &= \rho_\mu(p)\Gamma_\mu^{\rho\rho'}e^{ip(\rho-\rho')}+\lambda(p)\delta^{\rho\rho'} \\ \rho_\mu(p) &= \frac{i\alpha_\mu(p)}{\alpha_\mu^2(p)+\beta^2(p)}\ ;\quad \lambda(p)=\frac{\beta(p)}{\alpha_\mu^2(p)+\beta^2(p)}\ . \end{aligned} \tag{2.13}$$

[3] This is in contrast to Wilson-like fermions, where a chiral symmetry breaking smearing parameter is required for a local FPA [13].

The function $\rho_\mu(p)$ is antisymmetric and 2π antiperiodic in p_μ. In all other momentum components it is symmetric and 2π periodic, and the same holds for $\lambda(p)$ in all components of p. Hence we can expand these functions in Fourier series,

$$\rho_\mu(p) = \sum_z \rho_{\mu,z} e^{ipz} \ , \quad \lambda(p) = \sum_{n \in \mathbb{Z}^d} \lambda_n e^{ipn} \ , \tag{2.14}$$

where $z_\mu \in \{\pm 1/2, \pm 3/2, \ldots\}$ and $z_\nu \in \mathbb{Z}$, $\nu \neq \mu$. There is a symmetry under permutation and sign flip of λ_n in all components of n, and of $\rho_{\mu,z}$ in all z_ν, $\nu \neq \mu$. Furthermore $\rho_{\mu,z}$ is antisymmetric in z_μ.

Expressed in these quantities, the staggered fermion action takes the form

$$\begin{aligned} S[\bar{\chi}, \chi] \ &= \ \sum_{x \in \mathbb{Z}^d} \bar{\chi}_x^\rho \Big\{ \sum_{\mu,z} \rho_{\mu,z} \sigma_\mu(x) [\delta^{\rho - \hat{\mu}/2, \rho'} \chi^{\rho'}_{x+z+\hat{\mu}} + \delta^{\rho+\hat{\mu}/2,\rho'} \chi^{\rho'}_{x+z}] \\ &\quad + \sum_n \lambda_n \chi^{\rho'}_{x+n} \Big\}. \end{aligned} \tag{2.15}$$

The couplings for standard staggered fermions are

$$\rho_{\mu,z} = (\delta_{2z_\mu,1} - \delta_{2z_\mu,-1}) \prod_{\nu \neq \mu} \delta_{z_\nu,0} \ ; \quad \lambda_n = 2m \ \delta_{n,0} \ . \tag{2.16}$$

For the perfect action, defined in eqs. (2.9)–(2.12), the largest couplings are given in Table 1 and 2 for masses $m = 0,\ 1,\ 2$ and 4, and their decay is plotted in Fig. 1 and 2. We observe an extreme degree of locality, which is very important for practical purposes. For numerical application the perfect action has to be truncated to a short range. This truncation ought to alter the action as little as possible, in order to preserve the perfect properties to a good approximation.

3 Spectral and thermodynamic properties of perfect staggered fermions

Now we want to address the question, in which sense the action derived in section 2 is perfect, i.e. which observables are free of artifacts due to the finite lattice spacing.

First we look at the spectrum. For momentum $p = (\vec{p}, p_4)$ we see that the propagator has a pole at $p_4 = i\sqrt{\vec{p}^2 + m^2}$, which corresponds to the *exact*

(z_1, z_2, z_3, z_4)	$m = 0$	$m = 1$	$m = 2$	$m = 4$
(1/2,0,0,0)	0.6617391	0.5649324	0.3586038	0.0730572
(1/2,0,0,1)	0.0441181	0.0335946	0.0154803	0.0011324
(1/2,0,1,1)	0.0046569	0.0032407	0.0012088	0.0000711
(1/2,1,1,1)	0.0004839	0.0003251	0.0001282	0.0000114
(1/2,0,0,2)	0.0018423	0.0012135	0.0003688	0.0000063
(1/2,0,1,2)	0.0001419	0.0000741	0.0000096	-0.0000001
(1/2,1,1,2)	-0.0000264	-0.0000197	-0.0000065	-0.0000001
(1/2,0,2,2)	-0.0000145	-0.0000117	-0.0000046	-0.0000001
(1/2,1,2,2)	-0.0000126	-0.0000080	-0.0000022	0.0000000
(1/2,0,0,3)	0.0000780	0.0000445	0.0000090	0.0000000
(3/2,0,0,0)	0.0234887	0.0172839	0.0071677	0.0003303
(3/2,0,0,1)	-0.0004933	-0.0005804	-0.0004502	-0.0000389
(3/2,0,1,1)	-0.0009913	-0.0007019	-0.0002537	-0.0000067
(3/2,1,1,1)	-0.0004819	-0.0003056	-0.0000832	-0.0000009
(3/2,0,0,2)	-0.0001210	-0.0000924	-0.0000366	-0.0000008
(3/2,0,1,2)	-0.0001011	-0.0000623	-0.0000155	-0.0000001
(3/2,1,1,2)	-0.0000462	-0.0000255	-0.0000048	0.0000000
(3/2,0,2,2)	-0.0000129	-0.0000073	-0.0000015	0.0000000
(5/2,0,0,0)	0.0009439	0.0006010	0.0001648	0.0000018
(5/2,0,0,1)	-0.0000600	-0.0000483	-0.0000197	-0.0000003
(5/2,0,1,1)	-0.0000577	-0.0000339	-0.0000070	0.0000000
(5/2,1,1,1)	-0.0000187	-0.0000087	-0.0000007	0.0000000
(7/2,0,0,0)	0.0000390	0.0000215	0.0000039	0.0000000

Table 1: The largest kinetic couplings $\rho_1(z)$ for the optimally local, perfect staggered fermion of mass 0, 1, 2 and 4. The table contains all the couplings $\geq 10^{-5}$.

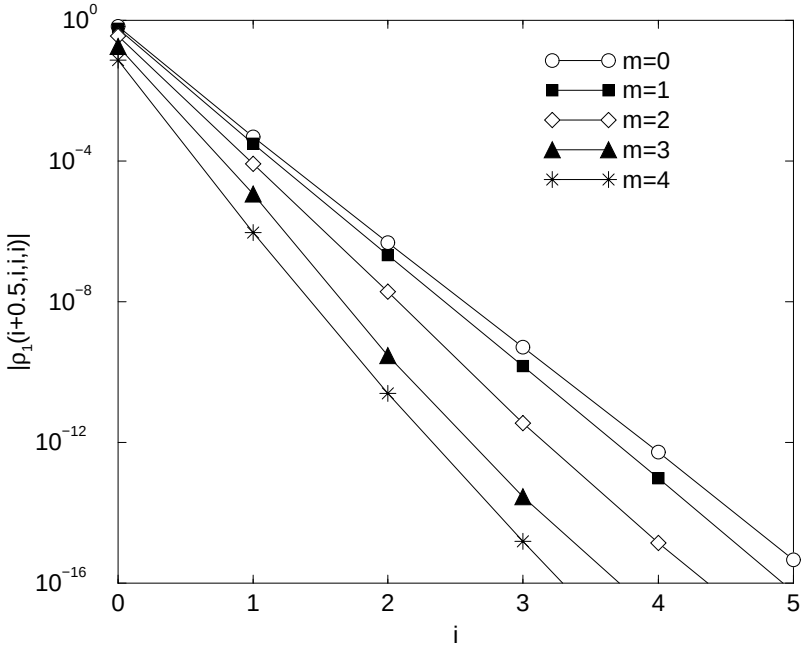

Figure 1: The decay of the kinetic couplings $\rho_1(i + 1/2, i, i, i)$ of the perfect staggered fermion for masses 0, 1, ... 4. We observe that the decay is exponential and very fast. For increasing mass it decays even faster.

continuum spectrum. We note that the Π function and the smearing term do not affect the singularity structure of the propagator. However, there are more poles — one for each $\vec{l}$ — namely [4]

$$p_{4,\vec{l}} = i\sqrt{(\vec{p} + 2\pi\vec{l})^2 + m^2} \ . \tag{3.1}$$

These poles correspond to higher branches. [5] Additional branches are necessary for perfection, since the lattice imposes 2π periodicity.

[4]Note that $\int_{-\pi}^{\pi} dp_4$ and the sum over l_4 combine to $\int_{-\infty}^{\infty} dp_4$.

[5]Sometimes higher branches are referred to as "ghosts", which should not be confused, however, with Faddeev-Popov ghosts.

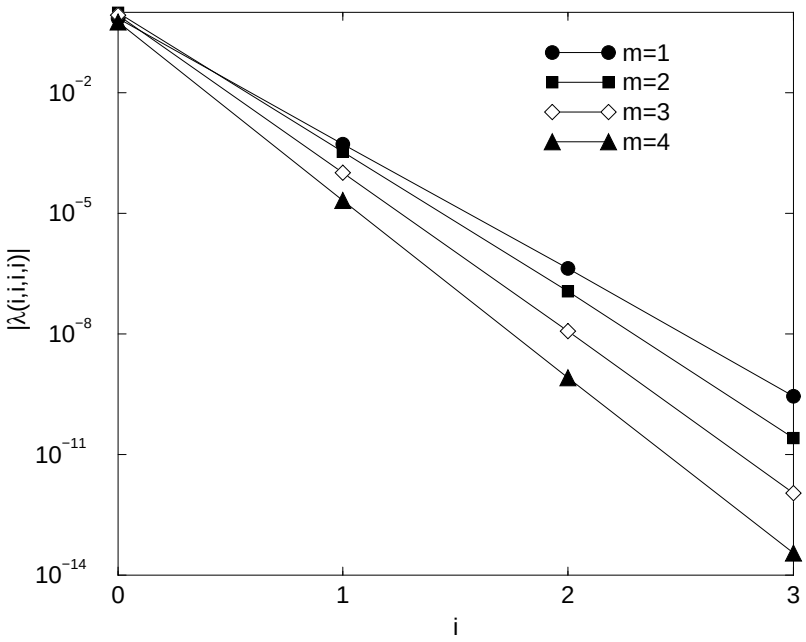

Figure 2: The decay of the static couplings $\lambda(i,i,i,i)$ in the perfect staggered fermion action at masses 1, 2, 3 and 4. We confirm that the decay is exponential and very fast, especially for large masses.

As a test case for truncated perfect fermions, it is interesting to observe how much harm we do to the spectrum – in particular to its lowest branch – if we restrict the couplings to a short range. In Fig. 3 we show the spectrum for a truncated perfect fermion, where we omit all couplings beyond $\pm 1/2, \pm 3/2$ in the μ direction for ρ_μ, and all couplings beyond $0, \pm 1$ in the non-μ directions of ρ_μ and in all directions of λ. The lower branch is real and approximates the exact dispersion relation better than the standard staggered fermion action, and the upper branch is the real part of two complex conjugate poles of the propagator.

An on-shell improved staggered fermion was proposed by S. Naik [14].

(z_1, z_2, z_3, z_4)	$m = 0$	$m = 1$	$m = 2$	$m = 4$
(0,0,0,0)	0	0.7091500	0.9799873	0.5705389
(0,0,0,1)	0	0.0296055	0.0246899	0.0034779
(0,0,1,1)	0	-0.0010357	-0.0015531	-0.0003674
(0,1,1,1)	0	-0.0012092	-0.0009711	-0.0000904
(1,1,1,1)	0	-0.0005181	-0.0003371	-0.0000208
(0,0,0,2)	0	0.0009257	0.0005581	0.0000181
(0,0,1,2)	0	-0.0000828	-0.0000703	-0.0000035
(0,1,1,2)	0	-0.0000567	-0.0000265	-0.0000003
(1,1,1,2)	0	-0.0000136	-0.0000026	0.0000001
(0,0,0,3)	0	0.0000332	0.0000133	0.0000001

Table 2: The largest static couplings $\lambda(z)$ for the optimally local, perfect staggered fermion of mass 1, 2 and 4. The table contains all the couplings $\geq 10^{-5}$.

By changing the kinetic term of the standard action (2.16) to

$$\rho_{\mu,z} = \Big(\frac{9}{8}[\delta_{2z_\mu,1} - \delta_{2z_\mu,-1}] - \frac{1}{24}[\delta_{2z_\mu,3} - \delta_{2z_\mu,-3}]\Big) \prod_{\nu\neq\mu} \delta_{z_\nu,0} \ , \qquad (3.2)$$

he removed the $O(a^2)$ artifacts for the free fermion. These couplings have no similarity to our perfect fermion. For comparison, the resulting dispersion relation is also shown in Fig. 3. By construction, this dispersion relation is good at $|p| << 1$, but at $|p_\mu| \sim 1$ the lower branch is hit by an upper branch, and then they turn into two complex conjugate poles, the real part of which is shown in the figure.

With respect to certain other quantities, even our untruncated action is not exactly perfect. When we performed the Gaussian integrals in the RGT (2.7), we did not keep track of "constant factors", which do not depend on the lattice fields. However, such factors may depend on other quantities such as the temperature. If those quantities are important – which was not the case in the spectrum – we can not expect perfect observables. Then one notices that the lattice fields are not completely renormalized. The possibility to keep track of such factors in a block spin RGT was explored for the Ising model in Ref. [15].

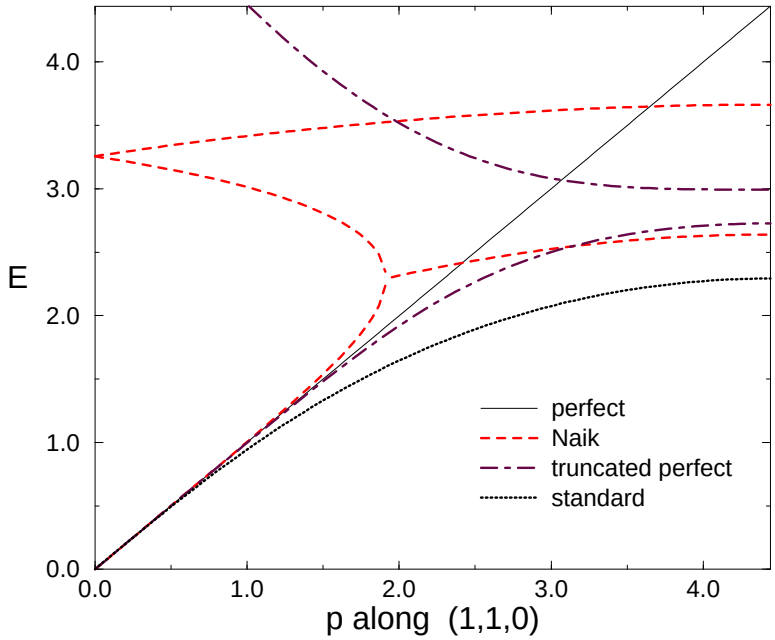

Figure 3: Dispersion relation for truncated perfect, Naik and standard, staggered fermions along (1,1,0).

As an example we consider the pressure of free, massless fermions in infinite volume. In the continuum the relation

$$\frac{P}{T^4} = \frac{7\pi^2}{180} \simeq 0.3838 \tag{3.3}$$

is known, where P is the pressure and T the temperature (Stefan-Boltzmann law). In Fig. 4 we plot the ratio P/T^4 for the staggered FPA and for the Naik and standard and staggered action at $N_t = 2, 4, 6 \ldots 40$ lattice points in the 4-direction (N_t must be even to accommodate a complete set of pseudoflavors). The standard staggered action scales better than Wilson fermions, in agreement with the fact that their artifacts are of the second order in the lattice spacing, whereas the Wilson action is plagued by linear artifacts [6].

[6] For Wilson fermions the ratio P/T^4 has a peak ~ 1.9 at $N_t \sim 2, 3$ [8]. For a discussion

We also see that even for the FPA this scaling quantity differs from the exact continuum result. This deviation is due to a missing temperature dependent renormalization factor. However, the figure shows that this factor is typically very close to 1. It differs significantly only on immensely coarse lattices. Hence the scaling is considerably improved with respect to the standard lattice actions. This is still true after truncation (the same we used when discussing the spectrum), although the behavior gets somewhat worse. Truncation causes an overshoot, which indicates that the fermion moves closer to the standard formulation. For the Naik fermion we confirm some improvement as well. Its thermodynamic behavior has also been discussed in Ref. [17]. The dip in the beginning is very similar to the behavior of the D234 action [18] (the corresponding thermodynamic plot is given in [8]). Note that also the construction of those two on-shell improved fermions – Naik for the staggered and D234 for the Wilson type fermions – is very similar: in both cases additional couplings are added on the axes (which is not too promising for the restoration of rotational invariance). Finally, the spectrum is very similar too, the lowest branches are hit by a doubler and turn complex around $|p_\mu| \sim 1$.

4 A free fixed point gauge action consistent with staggered fermions

Perfect staggered fermions can only be used in QCD if we are able to couple them to fixed point gauge fields in a perfect way. This requires a blocking scheme for the gauge field, which is consistent with the blocking for staggered fermions. The consistency condition is based on gauge covariance.

Let's go back to a finite blocking factor n. When we block from a fine to a coarse lattice, it is convenient to fix a gauge for the fine lattice fields. However, this gauge fixing should be restricted to one block, in order to avoid long distance gauge dependence.

Following Ref. [10] we block such that all contributions to a coarse lattice variable have the same pseudoflavor, as it is illustrated in Fig. 5. If a coarse pseudoflavor lives on a site x', then we consider the hypercube n^d with center

of the artifacts in standard staggered fermions and an improvement program for its matrix elements, see [16].

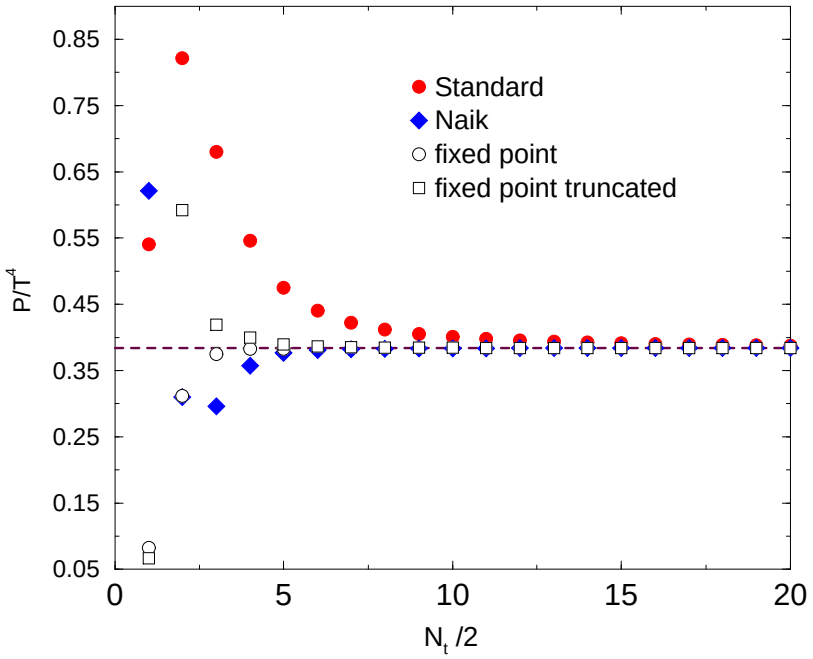

Figure 4: The thermodynamic scaling quantity P/T^4 for free massless staggered fermions with the standard action, the fixed point actions with and without truncation, and the Naik action.

x', and all the n^d fine variables of the same pseudoflavor contribute to that block variable. Thus each fine variable contributes to one coarse variable of the same pseudoflavor. (In the previous section we considered the limit $n \to \infty$ of this RGT.)

A coarse gauge field $A'_{\mu,x'}$ in terms of fine fields $A_{\mu,x}$, which is consistent with gauge covariance, is

$$A'_{\mu,x'+n\hat{\mu}/2} = \frac{b_n}{n^d} \sum_{x \in x'} \frac{1}{n} \sum_{j=0}^{n-1} A_{\mu,x+(2j+1)\hat{\mu}/2}, \tag{4.1}$$

where b_n is a constant renormalization factor. Its value is chosen such that we obtain a finite FPA for the free gauge field. Essentially, b_n neutralizes the constant factor from rescaling A'_μ, hence dimensional reasons suggest

$b_n = n^{d/2-1}$.

Here our fine lattice has spacing $1/2$ and the coarse one $n/2$, (n odd). The sum $x \in x'$ runs over all n^d fine lattice points that contribute to the coarse pseudoflavor living at the site x', and the lattice gauge fields live on the link centers. We sum over the straight connections of corresponding fine lattice pseudoflavors contributing to adjacent coarse lattice variables. This construction is illustrated for $n = 3$ in Fig. 5.

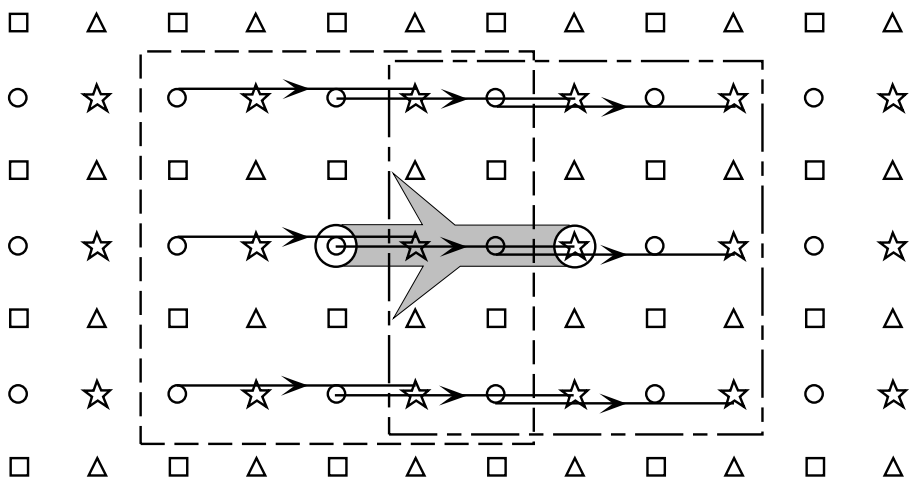

Figure 5: The staggered blocking of fermions and gauge fields, which maintains the pseudoflavor structure and gauge covariance. This figure illustrates the case $d = 2,\ n = 3$. Each symbol represents a pseudoflavor. Block variables are encircled and pick up contributions of the fine variables (with the same flavor) in the dashed box around them. The block link (shaded) is built from all the links covered by arrows.

In momentum space this condition reads

$$\begin{aligned} A'_\mu(p) &= \frac{b_n}{n^d} \sum_{l'} A_\mu(p + 4\pi l'/n) \Pi^M_{n\mu}(p + 4\pi l'/n)(-1)^{l'_\mu}, \\ \Pi^M_{n\mu} &= \frac{\Pi^M_\mu(np)}{\Pi^M_\mu(p)}\ , \quad \Pi^M_\mu(p) = \frac{4\sin(p_\mu/4)}{p_\mu}\Pi(p), \end{aligned} \tag{4.2}$$

where the summation extends over $l' \in \{0, 1, 2, \ldots, n-1\}^d$. Note that the momenta of the fine fields are in the zone $B_{4\pi} =]-2\pi, 2\pi]^d$, and those of the

coarse fields in $B_{4\pi/n} =]-2\pi/n, 2\pi/n]^d$. Since we defined the gauge variables on the link centers, $A_\mu(p)$ is 4π antiperiodic in p_μ.

Also here we want to send the blocking factor to infinity and block from the continuum. We start from a space-filling set of pseudoflavors, together with a continuum gauge field a_μ. In the limit $n \to \infty$ the above condition (4.1) turns into a Riemann integral of the form

$$\begin{aligned} A_{\mu,x} &= \int d^d y M_\mu(y) a_\mu(x-y) \\ M_\mu(y) &= \begin{cases} M(y_\mu) & |y_\nu| \le 1/2,\ \nu \neq \mu \\ 0 & \text{otherwise} \end{cases} \\ M(y_\mu) &= \begin{cases} 1 & |y_\mu| \le 1/4 \\ 3/2 - 2|y_\mu| & 1/4 \le |y_\mu| \le 3/4 \\ 0 & \text{otherwise} \end{cases} . \end{aligned} \tag{4.3}$$

This convolution is illustrated in Fig. 6. It is manifestly gauge covariant. Due to its architecturally interesting shape we call the function M_μ the *mansard* function.

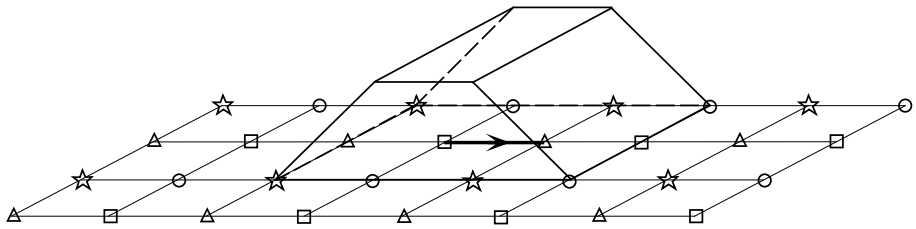

Figure 6: The "mansard blocking" of a gauge field from the continuum.

Note that

$$\int d^d y M_\mu(y) \exp(ipy) = \Pi^M_\mu(p), \tag{4.4}$$

and therefore condition (4.2) turns into

$$A_\mu(p) = \sum_{l \in \mathbb{Z}^d} a_\mu(p + 4\pi l) \Pi^M_\mu(p + 4\pi l)(-1)^{l_\mu}. \tag{4.5}$$

The following property can be understood from the above derivation, which started from a discrete RGT: if we perform a gauge transformation on an

Abelian gauge field, $a_\mu(y) \to a_\mu(y) + \partial_\mu\varphi(y)$, then the lattice gauge field transforms as $A_{\mu,x} \to A_{\mu,x} + \Phi_{x-\hat{\mu}/2} - \Phi_{x+\hat{\mu}/2}$, where $\Phi_x = \int_{c_x} d^dx\varphi(x)$ (c_x being a unit hypercube with center x). This shows gauge covariance and consistency with the fermionic blocking. The same properties were achieved in Refs.[6, 7] for fermions of the Wilson type, where the blocking was done by stepwise integration over disjoint cells and the gauge field was convoluted with a roof shaped function instead of the mansard function.

Now we construct the FPA, $S[A_\mu]$, for free gauge fields , which is adequate for staggered fermions. We impose the Landau gauge on the continuum gauge fields and choose the RGT

$$\begin{aligned}\exp\{-S[A_\mu]\} &= \int \mathcal{D}a\mathcal{D}D \exp\Big\{-\frac{1}{(2\pi)^d}\int d^dp\frac{1}{2}a_\mu(-p)p^2a_\mu(p)\Big\} \\ &\times \exp\Big\{-\frac{1}{(2\pi)^d}\int_{B_{4\pi}} d^dp\frac{1}{2}D_\mu(-p)[\alpha(p)+\gamma(p)\widehat{(p_\mu/2)}^2]D_\mu(p) \\ &+iD_\mu(-p)[A_\mu(p) - \sum_{l\in\mathbb{Z}^d} a_\mu(p+4\pi l)\Pi^M_\mu(p+4\pi l)(-1)^{l_\mu}]\Big\}, \quad (4.6)\end{aligned}$$

where the measure $\mathcal{D}a$ contains the gauge fixing factor $\delta(\sum_\mu p_\mu a_\mu(p))$ Again we impose the blocking condition (4.5) only by a Gaussian involving a mass-like and a kinetic smearing term. D_μ is an auxiliary lattice field, defined on the same links as A_μ, in analogy to the fermionic auxiliary fields $\bar{\eta}, \eta$ in eq. (2.7). Performing the RGT (4.6) yields

$$\begin{aligned}S[A_\mu] &= \frac{1}{(2\pi)^d}\int_{B_{4\pi}} d^dp\frac{1}{2}A_\mu(-p)\Delta^g_\mu(p)^{-1}A_\mu(p) \\ \Delta^g_\mu(p) &= \sum_{l\in\mathbb{Z}^d}\frac{1}{(p+4\pi l)^2}\Pi^M_\mu(p+4\pi l)^2 + \alpha(p) + \gamma(p)\widehat{(p_\mu/2)}^2. \quad (4.7)\end{aligned}$$

This is the FPA in a special gauge that we call "fixed point lattice Landau gauge", where A_μ obeys

$$\sum_\mu \sin\frac{p_\mu}{4}\Delta^g_\mu(p)^{-1}A_\mu(p) = 0. \quad (4.8)$$

We follow the standard procedure to rewrite the FPA in a gauge invariant form and arrive at

$$S[A] = \frac{1}{(2\pi)^d}\int_{B_{4\pi}} d^dp\frac{1}{2}A_\mu(-p)\Delta^g_{\mu\nu}(p)^{-1}A_\nu(p),$$

$$\Delta^g_{\mu\nu}(p)^{-1} \;=\; \Delta^g_\mu(p)^{-1}\delta_{\mu\nu} - \frac{\sin(p_\mu/4)\Delta^g_\mu(p)^{-1}\Delta^g_\nu(p)^{-1}\sin(p_\nu/4)}{\sum_\lambda \sin^2(p_\lambda/4)\Delta^g_\lambda(p)^{-1}}. \quad (4.9)$$

This result is similar to the one obtained for the roof-like blocking in [6, 7]. There it was possible to choose the smearing parameters such that the FPA in $d = 2$ turned into the ultralocal plaquette action. This can also be achieved for the "staggered FPA" given in eq. (4.9).

In $d = 2$, the standard lattice Landau gauge implies

$$A_\mu(p) = i\epsilon_{\mu\nu}\frac{\sin(p_\nu/4)F(p)}{\sum_\lambda 4\sin^2(p_\lambda/4)} \;, \quad (4.10)$$

where F is the plaquette variable defined on the plaquette centers. Inserting this into eq. (4.9) for $d = 2$, we find

$$\begin{aligned} S[F] &= \frac{1}{(2\pi)^2}\int_{B_{4\pi}} d^2p \frac{1}{2} F(-p)\rho(p)F(p), \\ \rho(p)^{-1} &= 16[\sin^2\frac{p_1}{4}\Delta^g_2(p) + \sin^2\frac{p_2}{4}\Delta^g_1(p)] \\ &= \cos^2\frac{p_1}{4}\cos^2\frac{p_2}{4}\Big(1 - \frac{1}{6}(\widehat{p_1/2})^2)\Big)\Big(1 - \frac{1}{6}(\widehat{p_2/2})^2)\Big) \\ &\quad +4\alpha(p)[(\widehat{p_1/2})^2 + (\widehat{p_2/2})^2] + 8\gamma(p)(\widehat{p_1/2})^2(\widehat{p_2/2})^2. \quad (4.11) \end{aligned}$$

If we choose

$$\begin{aligned} \alpha(p) &= \frac{1}{16} + \frac{1}{24}\cos^2\frac{p_1}{4}\cos^2\frac{p_2}{4} \\ \gamma(p) &= -\frac{1}{128} - \frac{1}{288}\cos^2\frac{p_1}{4}\cos^2\frac{p_2}{4}, \end{aligned} \quad (4.12)$$

then we obtain $\rho^{-1}(p) = 1$, as desired. Taking this as a guide for higher dimensions suggests that the optimal choice for the RGT parameters is

$$\begin{aligned} \alpha(p) &= \frac{1}{16} + \frac{1}{24}\prod_{\nu=1}^{d}\cos^2\frac{p_\nu}{4} \\ \gamma(p) &= -\frac{1}{128} - \frac{1}{288}\prod_{\nu=1}^{d}\cos^2\frac{p_\nu}{4}. \end{aligned} \quad (4.13)$$

It is important that $\alpha(p) + \gamma(p)(\widehat{p_\mu/2})^2$ is always positive. This ensures that the functional integrals in the RGT (4.6) are well defined.

Indeed it turns out that this RGT yields a very local FPA in $d = 4$. The largest couplings are given in table 3 and the exponential decay is plotted in Fig. 7.

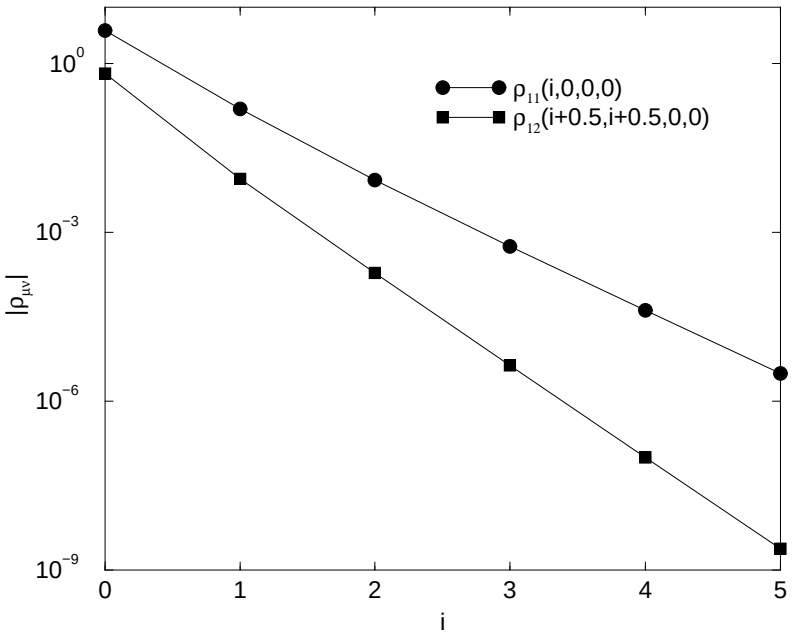

Figure 7: The exponential decay of the free gluon FPA for a RGT of the mansard type.

The dispersion relation of the transverse mansard gluon is again perfect, as it is the case for the perfect free fermion. If we truncate the couplings to distances $\leq 3/2$, we obtain the dispersion shown in Fig. 8. Due to our optimization of locality, the spectrum of the truncated fixed point gluon approximates the continuum spectrum still very well for small and moderate momenta. In practice, since these gauge fields are designed to couple to staggered fermions, the relevant momentum region is $|p_\mu| < \pi$, where the dispersion is quite good. We will find further evidence for this from the calculation of the quark-antiquark potential.

(z_1, z_2, z_3, z_4)	$\rho_{11}(z)$		(z_1, z_2, z_3, z_4)	$\rho_{12}(z)$
(0,0,0,0)	3.8112883		(1/2,1/2,0,0)	0.6609129
(0,0,0,1)	-0.3402240		(1/2,1/2,0,1)	0.0742258
(1,0,0,0)	-0.1541891		(1/2,3/2,0,0)	-0.0271129
(0,0,1,1)	-0.1150765		(1/2,1/2,1,1)	0.0148817
(1,0,0,1)	0.0508985		(1/2,3/2,0,1)	0.0047334
(0,1,1,1)	-0.0476001		(3/2,3/2,0,0)	0.0088456
(1,0,1,1)	-0.0058551		(1/2,3/2,1,1)	0.0015899
(1,1,1,1)	-0.0077244		(3/2,3/2,0,1)	-0.0003598
(0,0,0,2)	0.0054232		(3/2,3/2,1,1)	-0.0010820
(2,0,0,0)	0.0084881		(1/2,1/2,0,2)	-0.0041648
(0,0,1,2)	-0.0012443		(1/2,5/2,0,0)	0.0015083
(1,0,0,2)	-0.0065388		(1/2,1/2,1,2)	-0.0001960
(2,0,0,1)	-0.0039935		(1/2,3/2,0,2)	0.0004785
(0,1,1,2)	-0.0006582		(1/2,5/2,0,1)	-0.0005171
(2,0,1,1)	0.0011516		(3/2,5/2,0,0)	-0.0007231
(1,1,1,2)	0.0004326		(3/2,3/2,0,2)	-0.0002568
(2,0,0,2)	0.0011159		(3/2,5/2,0,1)	0.0001332
(1,0,2,2)	0.0005143		(3/2,3/2,1,2)	-0.0002152
(1,1,2,2)	0.0003562		(1/2,1/2,2,2)	0.0001109
(1,2,1,1)	0.0002912		(5/2,5/2,0,0)	0.0001907
(0,0,0,3)	-0.0005163		(1/2,1/2,0,3)	0.0002217
(3,0,0,0)	-0.0005617		(1/2,7/2,0,0)	0.0001005
(3,0,0,1)	0.0003064		(1/2,3/2,0,3)	-0.0001036

Table 3: The largest couplings for the fixed point action of the free gluon with respect to the "mansard RGT". The table includes all couplings in ρ_{11} with values $\geq 2.5 \cdot 10^{-4}$ and all couplings in ρ_{12} with values $\geq 10^{-4}$.

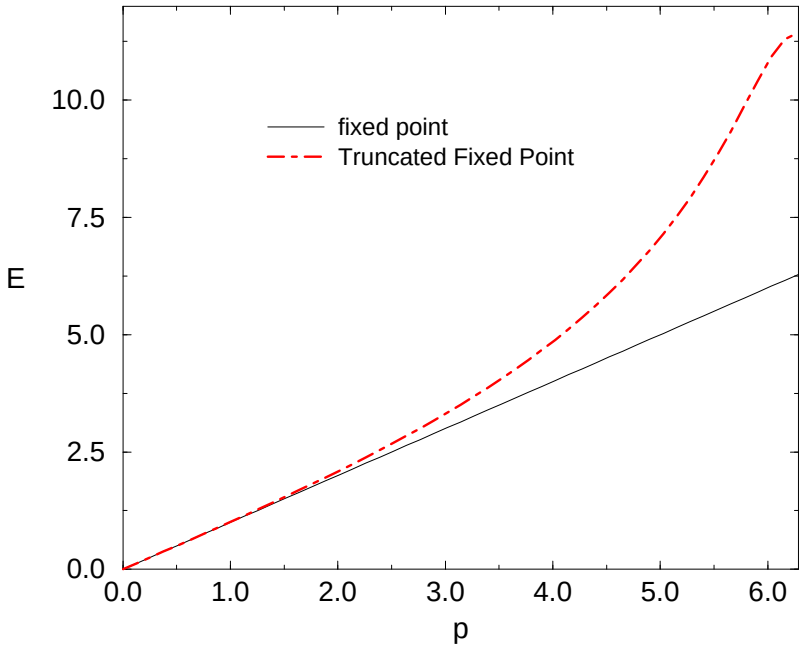

Figure 8: The dispersion relation of the truncated mansard fixed point gluon.

5 Polyakov loop and the static quark-antiquark potential

It is also possible to construct perfect operators for a given RGT. One adds a source term to the continuum action (or the fine lattice action) and includes this term perturbatively in the blocking process. In Ref. [3] the perfect $\bar{\chi}\chi$ operator was constructed in this way. In principle this method allows us to build any perfect composite operators, but in practice this tends to be difficult.

It is easier to construct "classically perfect" fields and operators. Classically perfect fields are obtained by minimizing the continuum action together with the blocking transformation term. If one inserts $\hbar$ in the RGT expression (4.6), then one obtains them in the limit $\hbar \to 0$.

For the free gauge field — and the RGT considered above — the classically

perfect field reads

$$a_\mu^c(p) = \frac{1}{p^2}\Pi_\mu^M(p)\Delta_\mu^g(p)^{-1}A_\mu(p), \tag{5.1}$$

where a_μ^c is in the Landau gauge and A_μ in the fixed point lattice Landau gauge. Note that classically perfect fields are defined in the continuum.

We obtain "classically perfect operators" from continuum operators if we replace the continuum fields by classically perfect fields, which are then expressed in terms of lattice fields. For instance, we can build a classically perfect Polyakov loop as

$$\phi^c(\vec{x}) = \int dx_d \; a_d^c(\vec{x}, x_d). \tag{5.2}$$

Inserting the gauge field given in eq. (5.1), we obtain in momentum space

$$\phi^c(\vec{p}) = \frac{1}{\vec{p}^2}\Pi_d^M(\vec{p},0)\Delta_d^g(\vec{p},0)^{-1}A_d(\vec{p},0). \tag{5.3}$$

Also this operator is defined in the continuum, in contrast to the standard lattice Polyakov loop $\Phi(\vec{p}) = A_d(\vec{p},0)$. Of course we can restrict the classically perfect Polyakov loop to lattice points by imposing 2π periodicity,

$$\Phi^c(\vec{p}) = \sum_{\vec{l}\in\mathbb{Z}^{d-1}} \frac{1}{(\vec{p}+2\pi\vec{l})^2}\Pi_d^M(\vec{p}+2\pi\vec{l},0)\Delta_d^g(\vec{p},0)^{-1}A_d(\vec{p},0). \tag{5.4}$$

In $d=2$ we found $\Delta_2^g(p_1,0)^{-1} = \hat{p}_1^2$, which leads to

$$\Phi_x^c = \frac{1}{4}(\Phi_{x+1} + 2\Phi_x + \Phi_{x-1}), \tag{5.5}$$

i.e. the classically perfect Polyakov loop is ultralocal on the 2d lattice. This confirms that the RGT parameters introduced in Sec. 4 optimize locality.

The correlation function of two classically perfect Polyakov loops,

$$\langle\phi^c(-\vec{p})\phi^c(\vec{p})\rangle = \frac{1}{(\vec{p}^2)^2}\Pi_d^M(\vec{p},0)^2\Delta_d^g(\vec{p},0)^{-1} \tag{5.6}$$

yields the static quark-antiquark potential

$$V(\vec{r}) = -\frac{1}{(2\pi)^{d-1}}\int d^{d-1}p \frac{1}{(\vec{p}^2)^2}\Pi_d^M(\vec{p},0)^2\Delta_d^g(\vec{p},0)^{-1}\exp(i\vec{p}\,\vec{r}). \tag{5.7}$$

In $d = 2$ this integral diverges as it stands. We subtract an infinite constant such that we obtain the correct behavior at large r. Then integration by contour techniques leads to

$$V(r) = \begin{cases} r/2 & r \geq 1.5 \\ (-32r^5 + 240r^4 - 720r^3 + 1080r^2 - 330r + 243)/960 & 1 \leq r \leq 1.5 \\ (32r^5 - 80r^4 - 80r^3 + 440r^2 - 10r + 179)/960 & 0.5 \leq r \leq 1 \\ (64r^5 - 160r^4 + 400r^2 + 178)/960 & 0 \leq r \leq 0.5 \end{cases} \tag{5.8}$$

This potential is shown in Fig. 9. It is very smooth (four times continuously differentiable) and coincides with the exact potential at $r \geq 1.5$.

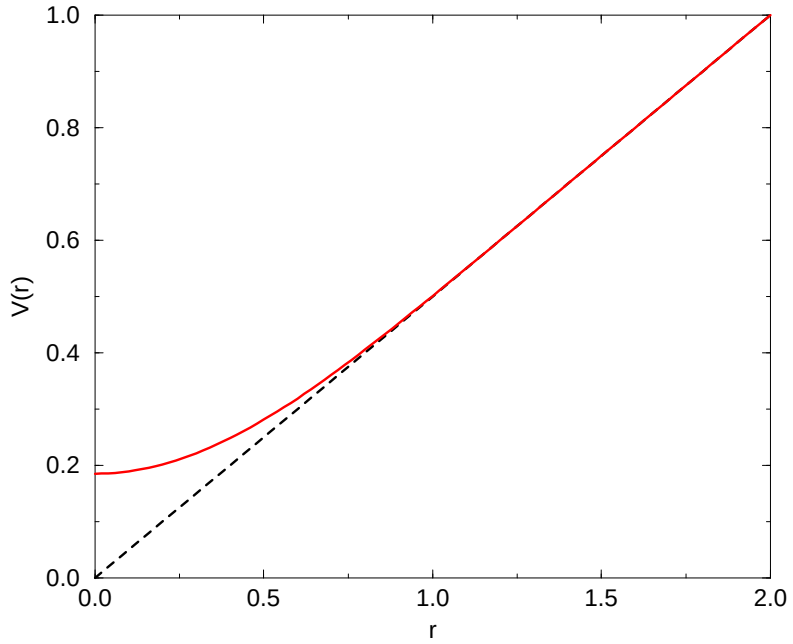

Figure 9: The classically perfect static quark-antiquark potential in $d = 2$.

In $d = 4$ the Fourier transform (5.7) has to be calculated numerically. The result is shown in Fig. 10 and compared to the static potential based on the standard lattice Polyakov loop, which is only defined if $\vec{r}$ is a lattice

vector. For the classically perfect potential, we observe a faster convergence of the scaling quantity $|\vec{r}|V(\vec{r})$ to the exact value $-1/4\pi$. Also rotational invariance is approximated much better, even down to $|\vec{r}| < 1$. The reason for the remaining artifacts in the classically perfect potential is related to the reason for imperfectness of the pressure discussed in Sec. 3. Here we also ignore "constant factors" in the Gaussian integrals of the RGT by taking just the minimum of the exponent. The remaining artifacts are exponentially suppressed.

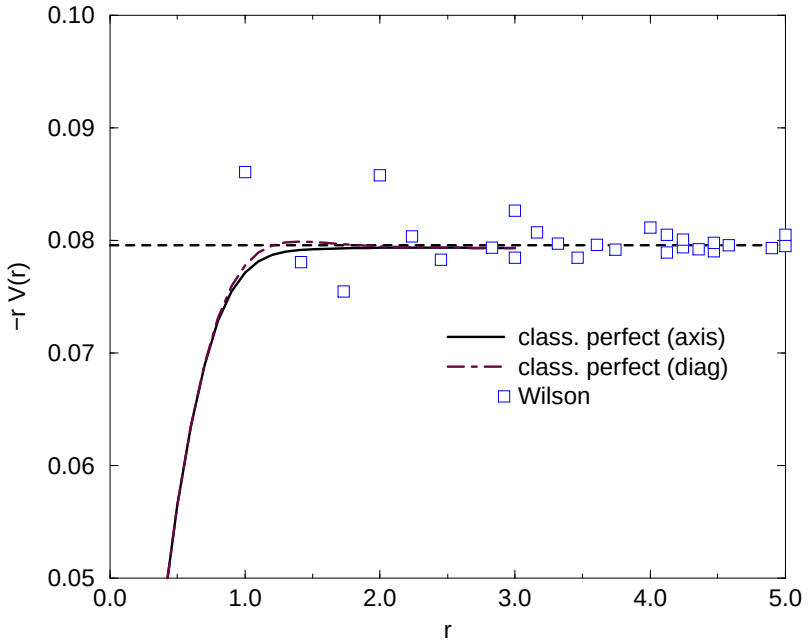

Figure 10: The classically perfect static quark-antiquark potential in $d = 4$ on an axis and on the space diagonal, compared to the potential obtained from Wilson's standard plaquette action.

6 Conclusions and outlook

We have constructed perfect free staggered fermions and perfect free gauge fields, which can be coupled consistently. This forms a basis for systematic perfect lattice perturbation theory, leading to a perturbatively perfect lattice action for QCD with staggered fermions. The next step is the evaluation of the perfect quark-gluon and the three gluon vertex functions as it was done for Wilson-like fermions [7, 8, 19]. In momentum space these vertex functions have almost the same form as written down in [7], with some modifications for staggered fermions and mansard gluons, which are obvious from the present paper. The lattice action thus obtained would be perfect for weak couplings. It may already be useful in lattice simulations even at moderate correlation length, since the classically perfect action is also expected to be one-loop perfect. The next step is to test the actions in simple situations. For example, one could study heavy quark physics, even though staggered fermions are not designed for such applications. In such a study, the worst artifacts of the standard lattice formulations originate from the large mass of the quarks. However, they are considerably suppressed for actions which are perfect at weak couplings. For Wilson fermions, we observed that even the use of the free perfect fermion action, together with standard lattice gauge fields, improves the mesonic dispersion dramatically [8] — although a large additive mass renormalization occurs. For staggered fermions, only a multiplicative mass renormalization will occur due to chiral symmetry.

An important aspect of staggered fermions is that they break the flavor symmetry when interacting with gauge fields. In lattice QCD with staggered fermions there is only one true "Goldstone pion". The other pions remain massive in the chiral limit, which manifests the flavor symmetry breaking [20]. This is a major obstacle in studying chiral symmetry breaking at finite temperatures, since the number of flavors plays an important role in such studies. In an experiment with a "fat link" — consisting of a link plus staples with varying staple weight — it was possible to reduce the mass of the remaining pions by about a factor two [21], which shows that there is a large potential for improvement by using non standard actions. However, the use of the Naik fermion does not seem to help here [22]. When we couple perfect staggered fermions and gauge fields consistently, we expect the flavor symmetry breaking to be strongly reduced. The "fat link" would naturally be incorporated. This could help to make the studies of chiral phase

transitions at finite temperature more realistic. As a simpler experiment one could combine the truncated perfect staggered fermion with a standard lattice gauge field. Perhaps this already helps to decrease the flavor symmetry breaking.

In principle, if the dynamics of the problem involve large gauge fields, as is obviously true for the physics of the light pions, it is unclear if the improvements obtained perturbatively are sufficient at the typical couplings where simulations can be performed. The couplings obtained perturbatively could undergo further renormalizations and new couplings may arise.[7] In such a situation one has to resort to non-perturbative techniques in order to obtain the classically perfect action. In this case one rescales the QCD action with the gauge coupling g and looks for a fixed point – i.e. a classically perfect action – of the rescaled theory. This can be done numerically by real space RGT steps, using the parameters for RGTs with finite blocking factors given in the appendix. The perturbatively perfect action may serve as a promising point of departure for this iteration. Thanks to the asymptotic freedom at $g = 0$, such RGT steps only consist of minimization of the action on the fine lattice together with the transformation term. No (numerical) functional integration needs to be performed, which simplifies the task enormously. In practice one starts from an updated configuration on the coarse lattice and determines the minimizing fields on the fine lattice. In this way, the effects of strongly fluctuating field configurations can be incorporated.

Acknowledgment

One of us, W.B., thanks F. Karsch for useful comments.

[7] However, we would like to emphasize that the perturbatively perfect action will approach the scaling region must faster than standard actions.

Appendix

A Parameters for RGTs with finite blocking factors and the same fixed point

In the limit $g = 0$ (where we determine the FPA), the quarks decouple from the gauge fields, hence we can start by constructing a pure gauge FPA. Here we provide the analytic ingredients for this purpose.

In Sec.4 we derived a FPA for free gauge field, which is consistent with the gauge requirements of staggered fermions. There we blocked from the continuum, but of course the same FPA can also be obtained using finite blocking factor RGTs. The optimal RGT parameters, which provide ultralocality in $d = 2$ and extreme locality in higher dimensions, depend on this blocking factor n (n odd). So far we only gave those parameters at $n \to \infty$. In this appendix we are going to identify them for general n. This is needed for the nonperturbative search of fixed points of non-Abelian gauge fields. There one does RGTs numerically, and is therefore restricted to finite blocking factors. In practice one would choose the smallest value $n = 3$.

Assume we are at the fixed point of Sec.4 in the fixed point lattice Landau gauge, and we perform a block factor n RGT,

$$\begin{aligned}\exp\{-S'[A'_\mu]\} &= \int \mathcal{D}A\mathcal{D}D \exp\{-S[A_\mu]\} \\ &\times \exp\Big\{ -\Big(\frac{n}{2\pi}\Big)^d \int_{B_{4\pi/n}} d^dp\ \frac{1}{2} D_\mu(-p)\Omega_{\mu,n}(p)D_\mu(-p) \\ +iD_\mu(-p)\Big[A'_\mu(p) - \frac{b_n}{n^d}\sum_{l'} A_\mu(p+4\pi l'/n)\Pi^M_{n\mu}(p+4\pi l'/n)(-1)^{l'_\mu}\Big]\Big\}, \quad \text{(A.1)}\end{aligned}$$

where $l' \in \{0, 1, 2, \ldots, n-1\}^d$ as in condition (4.2), which is (smoothly) implemented here. For the smearing term $\Omega_{\mu,n}$ we need an ansatz, which involves more parameters than it was the case for the blocking from the continuum,

$$\begin{aligned}\Omega_{\mu,n}(p) &= \alpha_n + 4\sin^2(np_\mu/4)\gamma_n + \sin^2(np_\mu/2)\omega_n \\ &\quad +[\delta_n + 4\sin^2(np_\mu/4)\sigma_n]\prod_{\nu=1}^d \cos^2(np_\nu/4). \qquad \text{(A.2)}\end{aligned}$$

The RGT parameters $b_n,\ \alpha_n,\ \gamma_n,\ \omega_n,\ \delta_n$ and σ_n can now be determined from the condition that the action be invariant under this RGT. Doing this integral and rescaling the coarse lattice momenta into the full zone $B_{4\pi}$, we obtain

$$\begin{aligned} S'[A'_\mu] &= \exp\Big\{ -\frac{1}{(2\pi)^d}\int_{B_{4\pi}} d^dp \frac{1}{2} A'_\mu(-p)\Delta^{g\,\prime}_\mu(p)^{-1} A'_\mu(p)\Big\}, \\ \Delta^{g\,\prime}_\mu(p) &= \frac{b_n^2}{n^d}\sum_{l'} \Delta^g_\mu((p+4\pi l')/n)\Pi^M_{n\mu}((p+4\pi l')/n)^2 + \Omega_{\mu,n}(p). \end{aligned} \tag{A.3}$$

We combine the sum over $4\pi l'/n$ with the sum over $4\pi l,\ l \in \mathbb{Z}^d$, which is intrinsic in Δ^g_μ, to a sum over $4\pi\ell/n,\ \ell \in \mathbb{Z}^d$. After doing some lengthy algebra and evaluating a number of trigonometric sums, we find that the fixed point condition $\Delta^{g\,\prime}_\mu(p) = \Delta^g_\mu(p)$ is fulfilled if

$$\begin{aligned} b_n^2 &= n^{d-2}\ , \\ 2\alpha_n &= 3\delta_n = 8n^2\omega_n = \frac{n^2-1}{8n^2}\ , \\ 4\gamma_n &= 9\sigma_n = -\frac{(n^2-1)^2}{32n^4}\ . \end{aligned} \tag{A.4}$$

We see that $\Omega_{\mu,n}(p)$ is always positive, such that $\int \mathcal{D}D$ is well-defined. In particular, we confirm the result for b_n, which we anticipated in Sec.4 by dimensional reasons, and in the limit $n \to \infty$ we reproduce the parameters for the blocking from the continuum obtained in eq. (4.12). As a further check we notice that $n = 1$ yields a trivial identity transformation, as it should.

References

[1] K. Wilson and J. Kogut, Phys. Rep. C12 (1974) 75.

[2] P. Hasenfratz and F. Niedermayer, Nucl. Phys. B414 (1994) 785.

[3] W. Bietenholz, E. Focht and U.-J. Wiese, Nucl. Phys. B 436 (1995) 385.

[4] T. DeGrand, A. Hasenfratz, P. Hasenfratz and F. Niedermayer, Nucl. Phys. B454 (1995) 587; 615.

[5] F. Farchioni, P. Hasenfratz, F. Niedermayer and A. Papa, Nucl. Phys. B454 (1995) 638.

[6] W. Bietenholz and U.-J. Wiese, Phys. Lett. B 378 (1996) 222.

[7] W. Bietenholz and U.-J. Wiese, Nucl. Phys. B464 (1996) 319.

[8] W. Bietenholz, R. Brower, S. Chandrasekharan and U.-J. Wiese, to appear in Proc. of LAT96 (hep-lat/9608068).

[9] W. Bietenholz and U.-J. Wiese, Nucl. Phys. B (Proc. Suppl.) 34 (1994) 516.

[10] T. Kalkreuter, G. Mack and M. Speh, Int. J. Mod. Phys. C3 (1992) 121.

[11] H. Dilger, hep-lat/9610029.

[12] G. Mai, Ein Bloskspin für $2^{d/2}$ Fermionen, diploma thesis, Hamburg (1989).
G. Mack, T. Kalkreuter, G. Palma and M. Speh, in "Lecture Notes in Physics" 409 (Springer, Berlin 1992), eds. H. Gausterer and C. Lang, p. 205.

[13] U.-J. Wiese, Phys. Lett. B315 (1993) 417.

[14] S. Naik, Nucl. Phys. B316 (1989) 238.

[15] M. Nauenberg and B. Nienhuis, Phys. Rev. Lett. 33 (1974) 944.

[16] A. Patel and S. Sharpe, Nucl. Phys. B395 (1993) 701; B417 (1994) 307.
Y. Luo, hep-lat/9604025.

[17] F. Karsch et al., to appear in Proc. of LAT96 (hep-lat/9608047).

[18] M. Alford, T. Klassen and G. P. Lepage, hep-lat/9611010.

[19] W. Bietenholz, R. Brower, S. Chandrasekharan and U.-J. Wiese, in preparation.

[20] C. Bernard and M. Golterman, Phys. Rev. D46 (1992) 853.
S. Sharpe, Phys. Rev. D46 (1992) 3146.
For reviews see e.g.
R. Gupta, Nucl. Phys. B (Proc. Suppl.) 42 (1995) 85.
D. Sinclair, Nucl. Phys. B (Proc. Suppl.) 47 (1996) 112.
and references therein. For a very recent work, see
S. Kim and S. Ohta, to appear in Proc. of LAT96 (hep-lat/9609023).

[21] T. Blum et al., hep-lat/9609036.

[22] C. Bernard et al., to appear in Proc. of LAT96 (hep-lat/9608102).